EPAC Laser Systems

N.H. Stuart, V. Aleksandrov, S. Buck, R. Heathcote, M. Galimberti, Y. Tang, I.O. Musgrave, P.D. Mason, P.J. Phillips, A. Wojtusiak, R. Heathcote, T. de Faria Pinto, R. Pattathil & C. Hernandez-Gomez
Central Laser Facility
STFC Rutherford Appleton Laboratory
Harwell Campus, Didcot
Oxfordshire OX11 0QX, UK

Overview

The Extreme Photonics Applications Centre (EPAC), under construction at the Harwell Campus in Oxfordshire (UK), will comprise a 1 PW laser operating at 10 Hz with two dedicated experimental areas housed in a stand-alone building. In order to achieve this high peak power and repetition rate, the laser system will comprise a Front End using Optical Parametric Chirped Pulse Amplification (OPCPA), and a main Ti:Sapphire amplifier pumped with a diode-pumped solid state laser (DPSSL). EPAC will use technology developed by the CLF for two revolutionary and unique DPSSL systems [1] that were supplied to the HiLASE Facility in the Czech Republic and the European XFEL in Hamburg (HiBEF). The CLF high-energy DPSSL technology is based on the so called 'DiPOLE' concept, that uses Yb:YAG cooled by cryogenic gas to enable efficient amplification of 10 ns pulses operating at 1030 nm to energies of up to 150 J at 10 Hz pulse rate (1.5 kW average power). Efficient wavelength conversion of DiPOLE systems into the green has also been demonstrated. In this report, we detail all the key parts of the EPAC laser system, whose linkages are shown in Figure 1. The layout of the laser subsystems on the second floor of the EPAC building is shown in Figure 2.

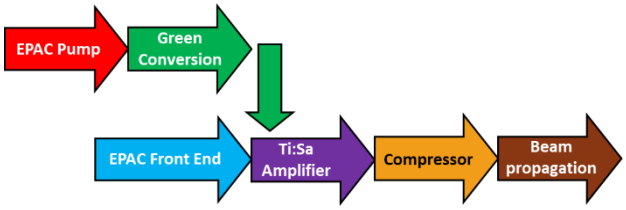

Figure 1: Concept of the EPAC laser system

Broadband, high energy and high-contrast 10Hz Front End for EPAC

The EPAC Front End supplies the pulses that seed the main High Energy Ti:Sa Amplifier. To that end, there are a number of key parameters that the Front End pulses must satisfy:

- The pulses must have sufficient bandwidth and energy to mitigate the expected reduction due to gain narrowing. For a Fourier-limited Gaussian pulse. the required bandwidth to support a 30 fs (FWHM) pulse is ~30 nm at 800 nm. To ensure that there is sufficient spectral content outside this, to prevent the introduction of contrast features due to fast spectral amplitude features and to give headroom to meet the 30 fs specification, the output from the front end will have a bandwidth of 110 nm.
- To minimise the amount of gain in the Ti:Sa amplifier, it requires an energy output of 1.5 J, equivalent to approx. 10^9 net energy gain from the ultrashort master oscillator seed source.
- Finally, the design needs to consider the impact of the Front End on contrast, by generating the initial ASE that will be amplified in the later stages of the system, through spectral phase noise imposed on the pulse during stretcher.

To satisfy these requirements, it has been decided to base the design of the EPAC Front End on the technique of OPCPA. It will comprise two sections of OPCPA amplification: the first section will be based in the picosecond time domain to amplify to >1 mJ and minimise the duration of any ASE [2]. The second section will be based on the nanosecond time domain to reach 1.5 J and maintain modest beam and optics sizes and low peak fluence through the amplifiers [3].

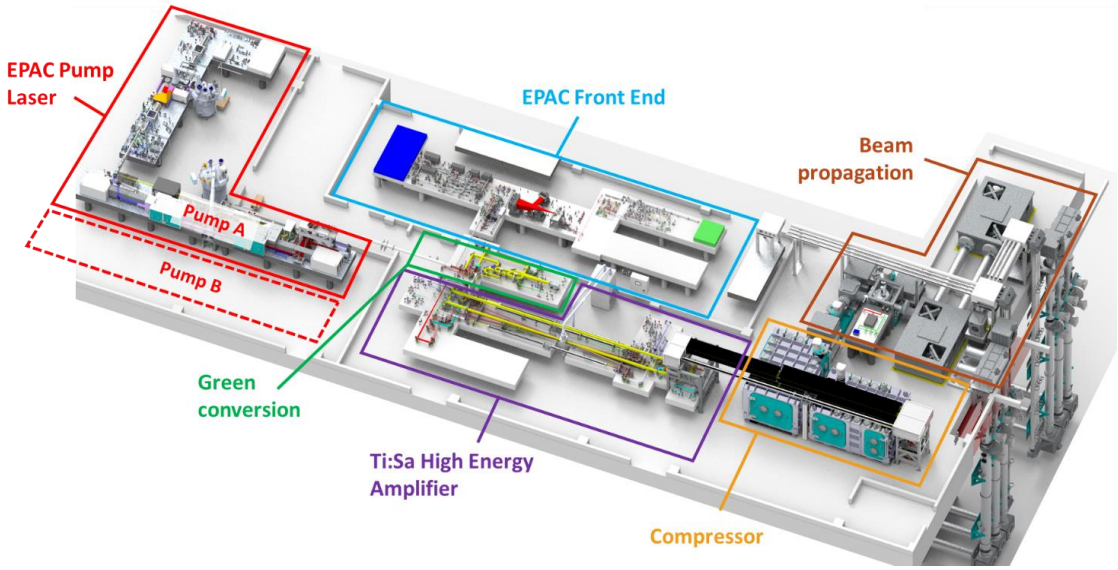

Figure 2: Layout of EPAC laser subsystems in the EPAC building

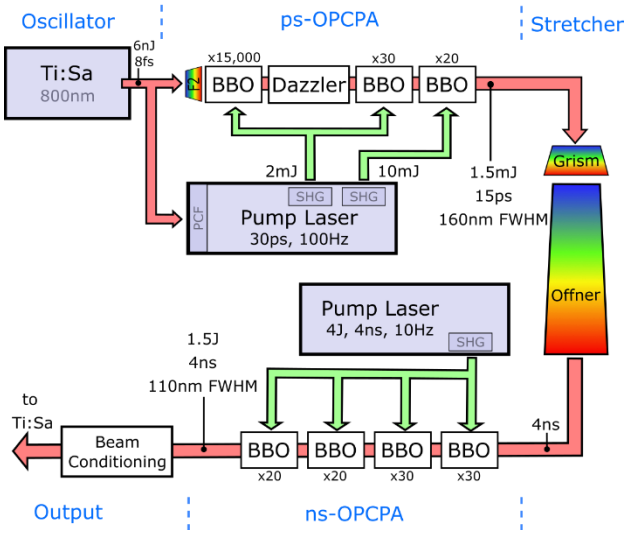

Figure 3: Schematic of the EPAC OPCPA Front End amplification sections

To prevent deleterious non-linear effects during amplification, the pulses need to be stretched in time. This will be achieved in a transmission grating-based stretcher scheme, after amplification to the millijoule level. The duration of the stretched pulse is based upon:

- the need to keep the overall accumulated B-integral to <1 rad.
- the separation and size of gratings feasible in the compressor.
- the capabilities of pump laser options for the nanosecond OPCPA.

As a result, it has been decided that the stretched pulse duration will be ~4 ns for the 110 nm bandwidth.

Picosecond-pumped OPCPAs (ps-OPCPA)

The design of the ps-OPCPA system is based on the one that has been developed for the Vulcan beamline OPCPA project (this has already demonstrated 1 mJ performance and has been compressed to <20fs) [4]. We have reviewed the design of the Vulcan system and have made a principle change to use a single pump laser to provide the pump pulses for all three of the ps-OPCPA stages, to minimise the temporal jitter between the seed and pump pulses. The pump laser will be commercially built 30 ps system that is optically synchronised to the signal pulse train, by seeding the pump laser from a portion of the seed beam and using a photonic crystal fibre (PCF) fibre to shift it to 1 µm.

The OPCPA stages will be seeded by the output of a Ti:Sa oscillator, which will be stretched to ~10 ps using high dispersion glass blocks (Schott N-F2). The oscillator will have the capacity to either be the master RF for the facility, or to synchronise to an external RF as required.

There will be a single stage of OPCPA before the beam passes through the acousto-optic programmable dispersive filter (AOPDF), enabling spectral phase control and compressibility optimisation for pulses in the experimental areas. Following the AOPDF, there will be two further stages of ps-OPCPA: the pulse duration in these stages will be slightly longer, due to the dispersion caused by the AOPDF.

BBO crystals will be used as the non-linear gain crystals. The amplifiers will operate at one-quarter of the quoted laser induced damage threshold of the AR coatings. With 10 mJ pump energy into the final stage, we expect more than the required 1.5 mJ signal energy with 160 nm FWHM bandwidth. This greater bandwidth overfills the spectral acceptance of the main stretcher to be resilient against temporal drifts of the picosecond pump laser. Each amplifier will accommodate a full set of diagnostics (near-fields, far-fields of pump and signal and spectrometer on the signal) alongside motorisation of the pump steering and phase-matching angle to facilitate remote monitoring and optimisation of amplifiers.

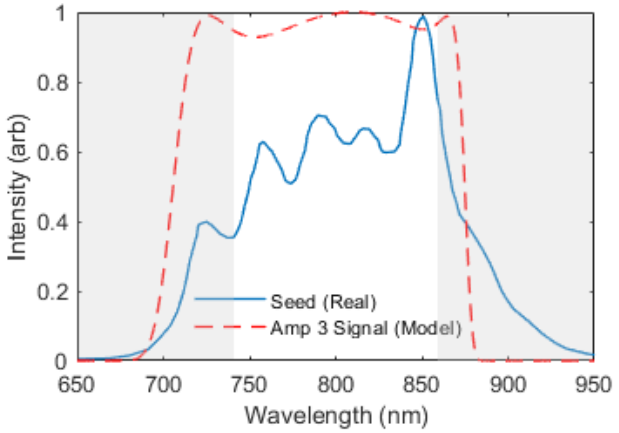

Figure 4: Key real and modelled spectra from ps-OPCPA modelling. Greyed area indicates rejected bandwidth edges through the stretcher and compressor sections.

The temporal contrast of the ps-OPCPAs fluorescence, using an additional source term (one photon per mode) into the 1D OPCPA models, predicts a contrast contribution of 6 x 10^9 at 10 ps ahead of the main pulse, as seen in Figure 5. This modelling was benchmarked in agreement to previous experimental data and found that fluorescence contrast is greatest when maximising the laser versus noise seed contrast in the first amplifier (i.e. small beam sizes) and operating the amplifiers in the saturated and pump depleted regime [5].

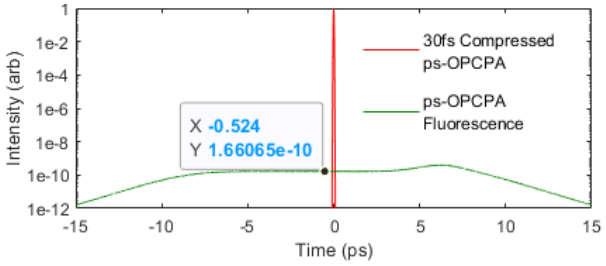

Figure 5: Modelled parametric fluorescence contrast of the ps-OPCPA design

Extra care has been taken to avoid sources of post-pulses that may couple into pre-pulse features through nonlinear couplings [6]. This includes adding slight non-parallel optic faces and elimination of near-collimated ghosts from telescope designs.

Stretcher scheme

The pulse stretching will be performed in two steps. The first stretcher is a tunable two-pass grism pair that will output between 70 and 120 ps pulses to enable compensation of material dispersion and pulse length tuning in experimental areas [7]. The second stretcher uses an Öffner imaging geometry to produce large amounts of chirp with minimal optical and spectral phase aberrations to produce a ~4 ns seed to the remaining amplifiers.

The optic configuration of the tunable stretcher is shown in Figure 6. The tunable stretcher will use transmissive diffraction gratings (DG) operating at Littrow angle with a roof mirror (RM) for beam extraction. In this scheme, it is possible for the large gratings and other large optics that comprise the main stretcher and compressor to be fixed and stable in their position to maintain alignment for long operational periods. As transmission gratings are used for the main stretcher to improve contrast [8], it was also necessary in the design to reduce the B-integral by increasing the pulse duration of the injected small beam into the main stretcher [9].

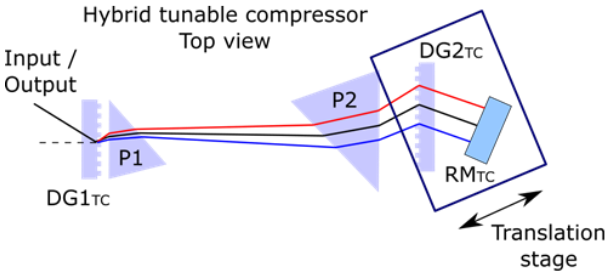

Figure 6: Layout of the grism tunable stretcher. The tunable stretcher will still use transmissive diffraction gratings (DG) operating at Littrow angle with a roof mirror (RM) for beam extraction.

The main stretcher uses a two grating optical setup in a four-pass reflective Öffner imaging geometry. The use of two gratings was found to be optimum for the very large stretch factor required to also minimise spherical aberrations. The convex and concave mirrors will be manufactured to have better than λ/250 RMS wavefront error and highest-grade polish to remove scatter sources that strongly degrade the temporal contrast of the laser pulse [10]. Figure 7 shows the top and side views of the main Offner stretcher that will stretch the pulses to ~4 ns. The convex mirror will have a radius of curvature (ROC) of 1.6m and that of the concave mirror will be -0.8m. The beams will be vertically separated within the stretcher by 15mm and will be injected 150mm away but parallel to the optical axis of the imaging system. To reduce the impact of surface imperfections on the laser contrast the input beam width to the stretcher will be 1.5mm such that the beam width on the concave mirror is ~0.5mm.

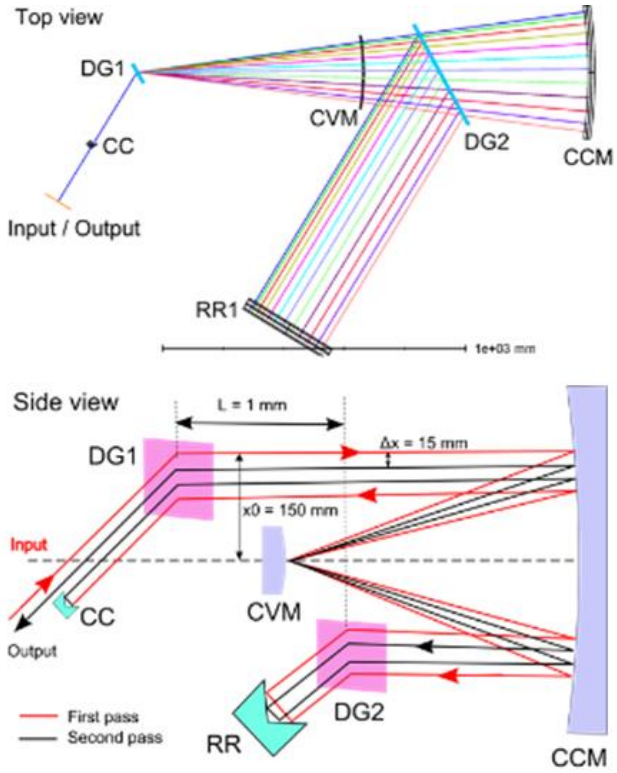

Figure 7: Top and side views of the main Offner stretcher

The combined dispersion of EPAC optics, stretcher and compressor systems and AOPDF incorporate compensation of up to fourth and fifth-order higher-order spectral phase aberrations, to ensure delivery of <30 fs and high-contrast pulses after the EPAC main compressor.

We also plan to draw a small amount of energy after the 2ns double-pass of the main stretcher to seed an independent Ti:Sa amplifier and compressor system for provision of probe pulses to the experimental areas.

Nanosecond-pumped OPCPAs (ns-OPCPA)

Four stages of OPCPA in the nanosecond regime have been designed to meet the 1.5 J output energy requirement to seed the Ti:Sa main amplifier. BBO has again been chosen as the amplifier medium to ensure a broad and uniform phase-matched bandwidth centred at 800 nm wavelength. A single electronically synchronised pump laser will be used to deliver 4 J, 4 ns pulses at 10 Hz repetition rate, with almost flat-top spatial and temporal profiles to ensure maximum energy extraction and bandwidth amplification across the 110 nm spectral window of the EPAC optical system.

In the nanosecond regime, reduced intensity thresholds for laser damage leads to smaller gain per BBO crystal length. Conversely, longer length crystals lead to spatial walk-off and beam profile inhomogeneities when using small, 1-5mm, beam diameters in the noncollinear pump-signal injection of the amplifiers, which is necessary to produce the broad bandwidth phase-matching. We have therefore limited the designed gain per stage to less than fifty, with the expectation that around 50-150 μJ of seed will be available from the stretcher. To avoid spatial walk-off issues, the first ns-OPCPA stage will use a short, 10mm length crystal, and is not expected to operate in the typical saturation regime, leading to marginal bandwidth and stability loss that is recovered in the following three stages. Walk-off compensation and saturation is then achieved after image inversion and amplification through the second stage when using similar beam sizes and crystal lengths.

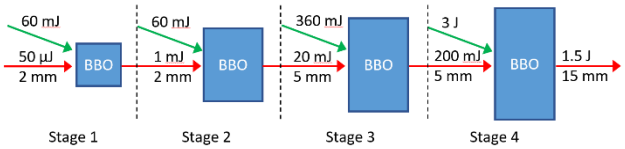

Figure 8: Schematic of the progression of the signal growth and pump energies for the ns-OPCPA section

Numerical modelling of the ns-OPCPA estimates a 1.5 J signal can be generated using 2.5 J pump energy into the final OPCPA amplifier stage, with energy headroom for beam imperfections and phase-mismatch in the upcoming implementation of the front end.

Output to the Ti:Sa Amplifier

For stability reasons it is anticipated that the front-end will routinely be operated at 10 Hz full energy. The output section of the front end will control the seed characteristics entering the Ti:Sa main amplifier to tailor operational requirements in the experimental areas.

Discrete and variable energy control throughout EPAC will be possible via energy attenuation mirrors and waveplates respectively. When switching between discrete attenuation steps, an optic of same material and thickness will always be present in the beam but of differing reflectivity to maintain the dispersion and position of the beam.

Isolation to prevent deleterious back reflections damaging the front-end components will be achieved using a Pockels cell & polariser. The repetition rate of pulses in the experimental areas will be controllable from single shot to 10 Hz via a fast-moving mirror to dump energy whenever pulses are not needed.

Mirrors of defined spectral reflectivity will also be used as static compensation of the non-uniform gain in the Ti:Sa main amplifier.

The image of the final ns-OPCPA crystal will be expanded and relayed onto the Ti:Sa gain medium using in-house designed achromatic doublet lens telescopes, which will minimise near-field alignment drift and maintain super-Gaussian beam profiles. The optical design of the twelve beam expansion telescopes has minimised chromatic aberration contributions on the broad bandwidth of the laser pulse wavefront to less than λ/20.

Conclusions

A detailed design of the EPAC Front End is now complete, with installation and commissioning planned during 2023 and verification of the pulse energy, bandwidth and compressed pulse duration the year after. The design meets the required energy, bandwidth and contrast commitments in a method suitable for stable year-round operations to provide a high quality seed to the Ti:Sa amplifier before compression to <30 fs to experimental areas.

EPAC Pump 120J DiPOLE Amplifier

Contact: jonathan.phillips@stfc.ac.uk

The EPAC pump laser is based on the CLF's DiPOLE amplifier technology and is the third 100 J-scale system that the CLF has produced to date. It will be the fourth kW-scale system, as we also have a parallel project developing a 100 Hz, 10 J system for our colleagues in HiLASE.

The EPAC DiPOLE 120 J laser is based on a master oscillator power amplifier (MOPA) incorporating multiple amplification stages as shown in Figure 9 and an isometric view of the system is shown in **Error! Reference source not found.**, showing the individual cryo amplifiers designs and also the layout of the rack room and the pump room.

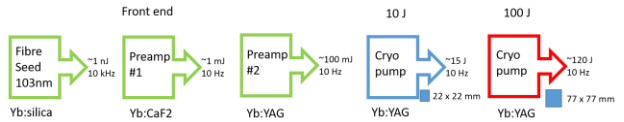

Figure 9: Schematic flow diagram of the EPAC DiPOLE 120 J

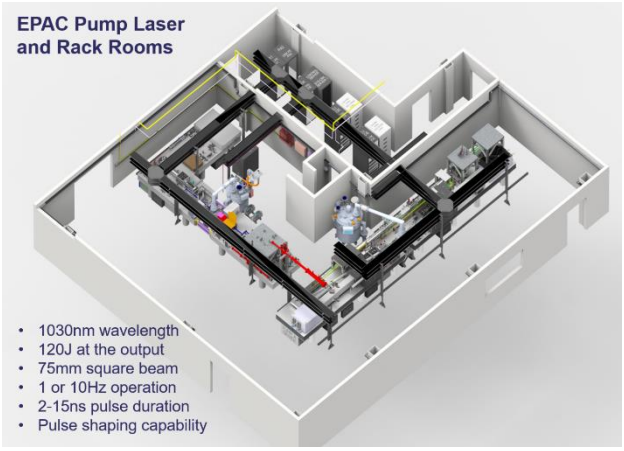

Figure 10: 3D CAD model

A general overview of the system is that a front end provides temporally (2 - 15 ns) and spatially (22 mm square flat top) flat shaped seed pulses with energies in excess of 100 mJ at 1029.5 nm. These pulses are then amplified to up to 15 J in a cryogenic pre-amplifier. The square output beam from the pre-amplifier is then expanded to a width of 77 mm before a final cryo-amplifier boosts the pulse energy to the 100 J-level. Both cryo-amplifiers are based on a multi-slab design, using Yb:YAG ceramic as their gain media, cooled by a high velocity stream of helium gas at cryogenic temperature, and employ a multi-pass architecture to extract the stored energy from the separate 940 nm pump diode sources. A more detailed description of the Front end 10 J Cryo amplifier and the 100 J amplifier follow.

Front end

The front end starts as a fibre seed source. This system contains an Arbitrary Waveform Generator (AWG), which provides the ability to shape the temporal pulse, and allows the system to operate with a pulse as short as 2 ns or as long as 15 ns, with the energy of the system restricted with shorter pulses to ensure the damage threshold is not exceeded. The output of the seed source is amplified in a commercial amplifier system to provide an output of approximately 4 mJ. A second commercial amplifier, which increases the energy of the beam to over 100 mJ, as is required to seed the 10 J cryoamplifier. The optical path within the front end converts the beam from a circular Gaussian to a square top hat beam. A number of diagnostics are deployed throughout the front end system, including near field and far field cameras, photodiodes as temporal diagnostics, and energy meters. A continuous wave (CW) system is also included to allow the alignment of the front end to be verified without the use of the pulsed laser systems.

10 J Amplifier

As with the previous three systems, the front end beam travels through the 10 J amplifier head seven times in an image-relayed multipass arrangement and a schematic of the system is shown in Figure 11. The Yb doped YAG ceramic disks will have chromium-doped cladding along the edge, to minimise ASE and suppress parasitic oscillations. There are four disks with two different doping concentrations: the two central disks have a higher doping concentration than the outer disks, in an arrangement chosen to equalise the gain and heat load.

The amplifier head can be thought of as two vessels; a pressure vessel within a vacuum vessel. The beam passes through a fused silica window into the vacuum vessel. A sapphire window forms the boundary between the vacuum vessel and the pressure vessel, with the gain media housed inside the pressure vessel. The pressure vessel allows the gain media to be cooled by the flow of helium that is itself cooled using liquid nitrogen in a cryostat. The pressure in this part of the head is 10 bar. The vacuum vessel isolates the pressure vessel from the outside environment, to ensure that no ice or condensation forms in or on the amplifier head.

The gain media contained in the amplifier head is pumped from both sides using laser diodes, which are capable of delivering a peak power of 29 kW with a duration of 1 ms. The wavelength of the diodes is 940 nm. In previous systems, a dichroic mirror has been used to inject this diode light into the amplifier head. This optic reflected the 940 nm light into the amplifier head while transmitting the 1030 nm seed beam. As these two wavelengths are similar, the coating requirements were difficult to achieve and prone to damage. In this system, we have, therefore, decided to remove the dichroic optic and replace it with a pump mirror optimised for the 940 nm light, and to move this optic to outside the seed beam path. To achieve this, the amplifier head has been rotated slightly, by 4 degrees, to the seed beam.

To keep the system as compact as possible, two large vacuum spatial filters are sited on either side of the amplifier head, rather than individual pipes for each pass of the amplifier head. An AO system will be deployed on the 10 J system, with the deformable mirror on the third pass, and the wavefront sensor deployed at the output of the system. The deformable mirror will be built in-house, with the wavefront sensor and control software purchased to ensure compatibility across the EPAC project.

Diagnostics will be deployed after each pass, with additional diagnostics deployed at the output of the 10 J cryoamplifier system, including a photodiode for temporal measurement and an energy meter. Additionally a dark field diagnostic is being deployed to detect damage to optics within the amplifier head. These optics are critical; they are also expensive and have a long lead time, so it is essential that they are monitored carefully during operation, which is possible through the darkfield diagnostic.

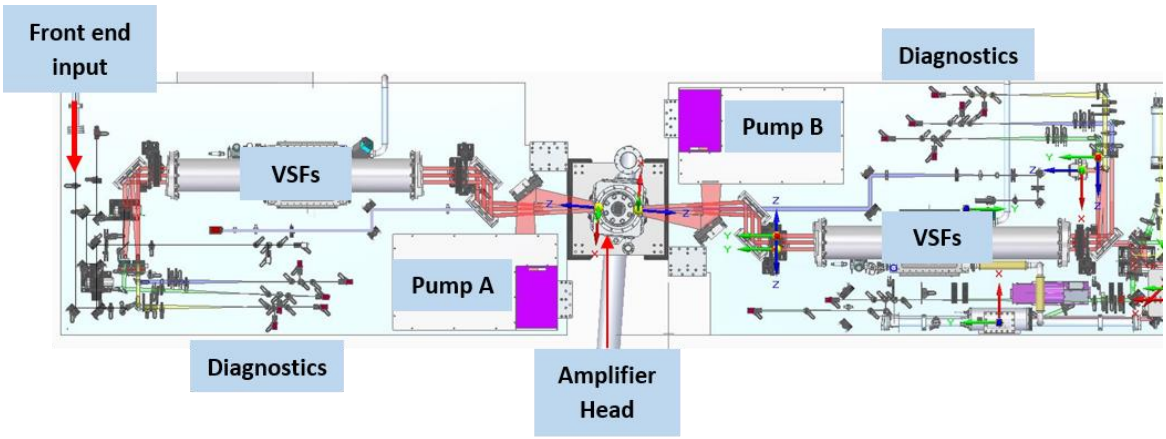

Figure 11: Schematic of 10 J system

The darkfield system has been successfully deployed on the previous two 100 J-level systems, and uses a pulsed 1030 nm laser that is timed asynchronous to the main laser pulse being amplified. On one side of the amplifier head, the darkfield optical path is constructed to generate a beam that is square and covers the same area in the amplifier head as the pump diode beam; this is defined as the main area of interest. On the other side of the amplifier is an imaging system, with a schlieren stop placed at the focus of a reducing telescope. Where there is no damage to the optics in the amplifier head, the camera image is black; anything causing the darkfield beam to scatter, such as damage or dust, will show as a bright spot on the camera image.

The beam propagates from the 10 J system to the 120 J system, and during this journey is expanded to a 75 mm square beam. A schematic of the setup is shown in Figure 12. A Faraday isolator is placed to protect the 10 J system from any back reflections from the 120 J system. The capability exists at this point to split the 10 J output into two separate beam lines, using two polarisers mounted at Brewster angle, with a series of waveplates earlier in the beam path allowing selection of the polarisation and, therefore, of the relative energy split into the two beam paths. Initially a single 120J amplifier stage will be built, but the design of the pump system future-proofs the system by allowing for the incorporation of an additional high energy amplifier to increase the energy available in the pump at a later date.

The control of the polarisation is critical for the 120 J system, and a series of waveplates has been deployed after the split into two beams to optimise the polarisation into the 120 J section. The beam travels to the 120 J table in a vacuum pipe, which is set at a height of over 2 m from the floor, to allow access to other areas of the system. The beam transport system has been optically modelled to ensure ghosts and stray light are terminated appropriately and CAD drawings exist to detail the parts required.

120 J Cryo Amplifier

To amplify the 10 J beam, the laser travels through the 120 J amplifier head four times in an image relayed multipass arrangement, as shown in Figure 13. There are six, square Yb-doped YAG gain media slabs in this system, with cladding along the outer edge to minimise ASE and suppress parasitic oscillations. There are three different doping concentrations: the two central slabs have the highest doping concentration and the outer most slabs have the lowest doping concentration, in an arrangement again chosen to equalise the gain and heat load. While there are more gain media slabs contained in this amplifier head, the general scheme is the same as for the 10 J system, with fused silica windows on the outside of the amplifier head, and sapphire windows providing the boundary between the pressure vessel and the vacuum vessel.

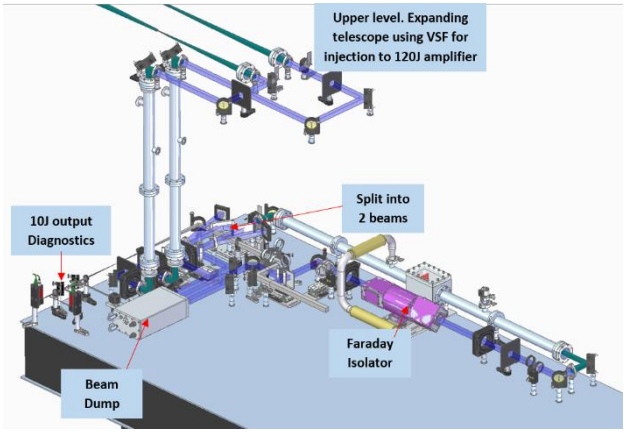

Figure 12: Schematic of the beam path from the output of the 10 J system to the 120 J input, showing the two levels. The 10J multipass has been removed to highlight the beam path to the 120J amplifier therefore the blank space in the foreground is not empty

The gain media contained in the amplifier head is pumped from both sides using laser diodes. In this system, we have chosen to increase the peak power capability to 350 kW. This increased headroom will allow us to extract more energy.

In this system, due to the size of the beams, a separate VSF is required for each pass. An AO system will be deployed, with the deformable mirror on the first pass and the wavefront sensor deployed at the output of the system. Diagnostics will be deployed across each pass, with additional diagnostics deployed at the output of the system. Additionally a dark field diagnostic has been deployed to detect damage to the optics within the amplifier head. These optics contained are critical; they are also expensive and have a long lead time, so it is essential that they are monitored carefully during operation, which is possible through the darkfield diagnostic. The darkfield diagnostic deployed for this amplifier is similar to the 10 J diagnostic described above; however, here the darkfield beam size is larger.

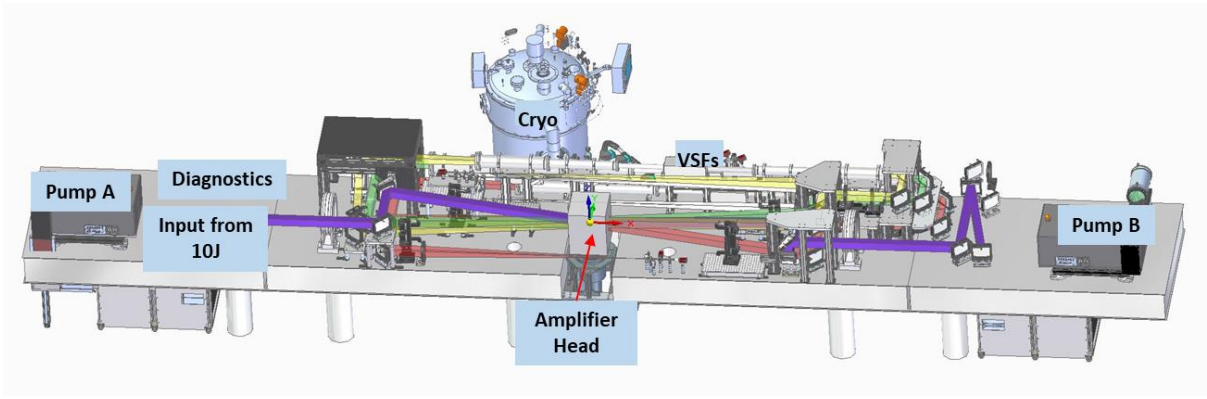

Figure 13: Schematic of the 120 J section of the pump laser system. The key commercial components are shown, as is the basic multipass design. The diagnostics and input from the 10 J system are not shown here.

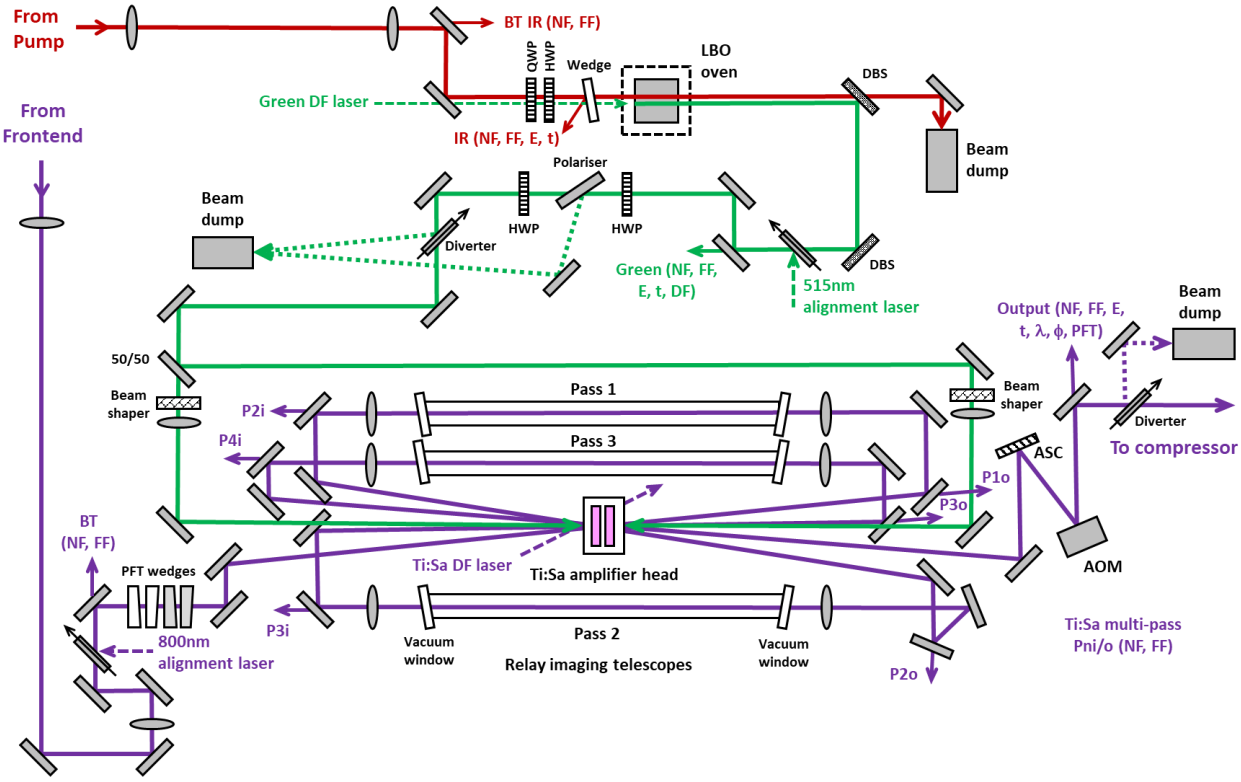

Figure 14: Schematic layout of EPAC Ti:Sa high energy amplifier. BT = Beam Transport, QWP = Quarter Wave Plate, HWP = Half Wave Plate, DF = Dark Field, NF = Near Field, FF = Far Field, E = Energy, t = temporal, λ = spectral, ϕ = wave front, DBS = Dichroic Beam Splitter, PFT = Pulse Front Tilt, AOM = Adaptive Optic Mirror, ASC = Astigmatism Corrector. P_n = Pass number (i = input direction, o = output direction).

Ti:Sa High Energy Amplifier

Contact: paul.mason@stfc.ac.uk

The Ti:Sa high energy amplifier is used to amplify the ns-scale stretched broad bandwidth output pulses from the EPAC Front End (see above). The design is based on a large aperture titanium-doped sapphire (Ti:Sa) amplifier head pumped from both sides by high energy 515 nm pump beams generated from the EPAC Pump laser system (see above). In the first phase of commissioning a single pump laser will be available with a second being added later for final commissioning of the system. Figure 14 (above) shows a schematic layout of the Ti:Sa high energy amplifier system, with single infrared (IR) pump and green beam path, and the Ti:Sa multi-pass architecture shown.

The pulsed 1030 nm IR beam from each pump laser will be down collimated in size to a 65 mm square beam before being relay-imaged into a green wavelength converter. Conversion to the green at 515 nm occurs using second harmonic generation (SHG) in a large-aperture (75 mm x 75 mm x 24 mm) LBO crystal. A combination of wave plates (quarter- and half-wave) before the crystal will ensure the correct input polarisation state for efficient Type I phase-matching. This configuration is expected to generate 80 J pulses at 515 nm after the SHG crystal from each pump laser with an efficiency of at least 70%. A wedge before the LBO crystal will provide a polarisation independent channel for input IR diagnostics (NF, FF pointing, energy and temporal). The LBO crystal will be housed in a temperature-controlled oven to ensure that conversion efficiency can be maintained over the range of pulse operating modes of the EPAC facility.

The generated 515 nm beam will then be separated from the unconverted IR beam by reflection from a pair of dichroic beam splitters (HR @ 515 nm, HT @ 1030 nm). A waveplate-polariser combination will provide the ability to independently control the pump energy delivered to the Ti:Sa amplifier. Small samples of the beam will be taken at various locations to provide 515 nm diagnostics (NF, FF pointing, energy and temporal). The generated green beam from each crystal will then be split into two beams of equal energy before being shaped from square to

circular, resized and imaged into the Ti:Sa amplifier head from opposing sides. Each pair of 515 nm beams will be injected off-axis at similar but opposing angles in a near-vertical plane to allow physical separation from the amplified beams. To ensure good overlap and uniform gain across the amplifier the 515 nm beam will be slightly larger (55 mm during phase 1 and 75 mm for final commissioning) than the circulating amplified beams. During initial commissioning, a total of 70 J green energy will pump the Ti:Sa amplifier, taking into account overlap and shaping losses, and any unabsorbed 515 nm radiation will be re-injected into the amplifier using a mirror-based recycling scheme to maximise efficiency. When both pump lasers are available the Ti:Sa amplifier will be pumped by four beams, two from each side, delivering a total energy of at least 125 J at 10 Hz.

The Ti:Sa amplifier head uses a modified version of the helium gas-cooled multi-slab architecture developed for the CLF family of DIPOLE high energy pump lasers. A pair of composite shaped Ti:Sa crystals (clear aperture 100 mm, thickness 20 mm) will be held in close proximity inside a pressure vessel and their temperature stabilised by flowing helium gas across their surfaces to remove heat and enable operation at pulse rates up to 10 Hz. A solid-state absorber cladding will be added to the edge of each crystal to reduce amplified spontaneous emission (ASE) to a manageable level and prevent undesirable parasitic oscillations. The Ti:Sa crystals will have a low titanium doping level to reduce transverse gain and further reduce the risk of detrimental ASE effects. The thickness of each slab is designed to provide 90% absorption of the 515 nm pump in a single pass through the amplifier head.

Before amplification, the circular super-Gaussian, spectrally shaped frontend output beam will be expanded by an achromatic beam expanding telescope. The magnification of the telescope and resulting beam size (52 mm during phase 1 increasing to 72 mm during final commissioning) has been chosen to ensure efficient energy extraction from the Ti:Sa amplifier (extraction fluence 1.3 J/cm²), whilst operating at safe energy densities to preserve components and allow long term operation of the facility.

After expansion the beam will pass through two pairs of complimentary glass wedges. The wedge angles can be independently adjusted to allow pre-compensation for pulse front tilt (PFT) so that it is minimised after propagation to the Experimental Areas.

To extract the stored energy in the Ti:Sa amplifier, the beam will be passed four times through the amplifier head with all passes in the same horizontal plane to maintain optimum polarisation orientation. This will be done using a bow-tie architecture, similar to that used on the CLF Gemini laser [11], with each pass at a different angle to minimise the risk of scatter from amplifier optics coupling into neighbouring passes, which could otherwise lead to unwanted pre/post pulses being generated. The beam is relay-imaged on each pass using achromatic relay-imaging telescopes, made using custom refractive air-spaced doublets, to aid alignment stability and ensure propagating beam quality is maintained. Because the length of each optical pass is slightly greater than 4F, the image plane from the input beam expanding telescope is set beyond the Ti:Sa amplifier. The relay-imaging telescopes then ensure that on each subsequent pass the image moves closer to the amplifier until it is imaged on to the amplifier after the final pass. A programmable astigmatism corrector (ASC) and an adaptive optic mirror (AOM) will be installed after the final pass through the amplifier to ensure good wave front quality is maintained for the different operating modes. The output beam will then be expanded and relay imaged to the pulse compressor.

A 3D CAD drawing of the Ti:Sa high energy amplifier system with the main system components highlighted is shown in Figure 15.

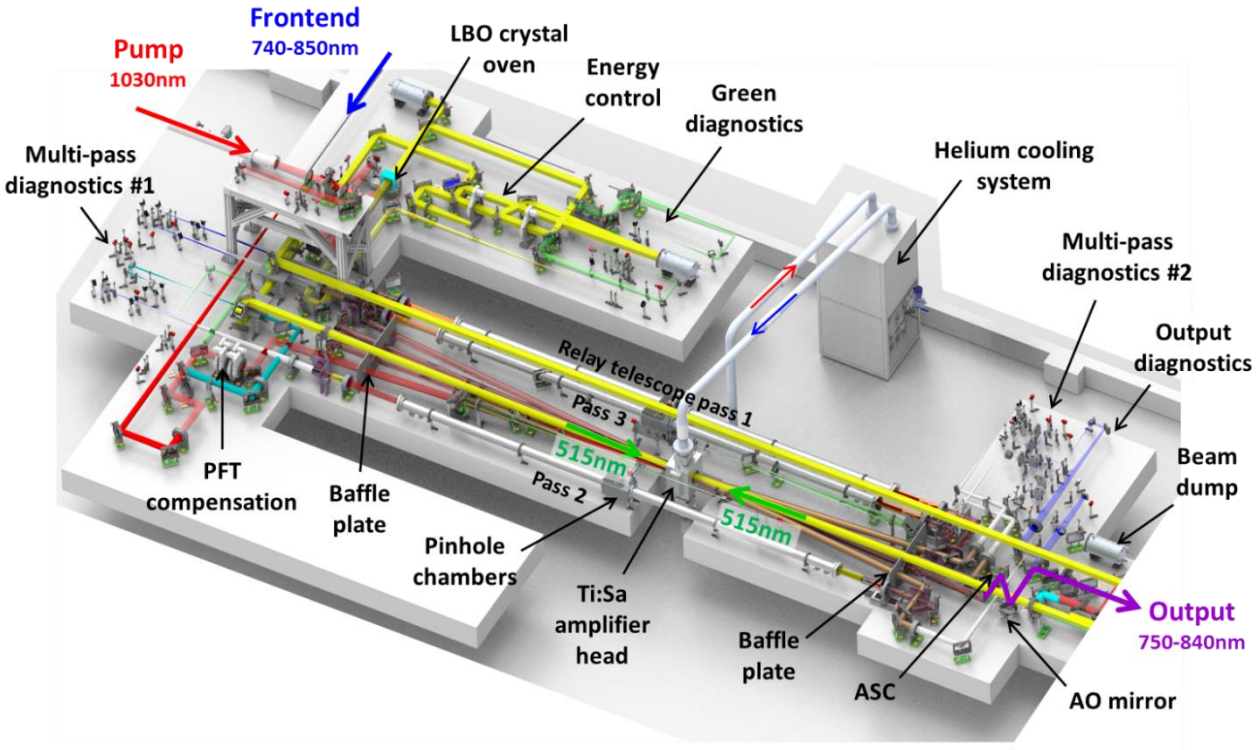

Figure 15: CAD drawing of EPAC Ti:Sa high energy amplifier system

EPAC Compressor

Contact: nick.stuart@stfc.ac.uk

Introduction

The EPAC compressor will shorten the duration of the high-energy laser pulses from 3 ns to ≤ 30 fs FWHM and output 1 PW pulses at up to 10 Hz repetition rate routinely to experimental areas.

The design of the EPAC compressor has been influenced by the work undertaken on other CLF projects, such as the Vulcan 20PW project [12], Vulcan OPPEL [13] and the Gemini laser facilities [14], all of which have been based upon the use of reflective diffraction gratings used at Littrow angle and out-of-plane to maximise efficiency and maintain easy access to the incoming and outgoing beams. Recent development work on diffraction grating design has also shown that the bandwidth of the diffraction efficiency for dielectric gratings is improved when operated in this geometry [15]. The Vulcan OPPEL and the Gemini compressor use a two-grating double-pass scheme, with the beams being displaced in the near-field for extraction. This near-field displacement is achieved using a retro reflecting mirror with a slight angle in the non-dispersion plane, which results in a residual spatial chirp to the beam and the propensity for pulse-front tilt. The EPAC compressor uses an improved geometry to remove this spatial chirp by using a four-grating scheme.

The internal layout and position of the compressor is shown in Figure 16. The compressor will be laid out as two sub-compressors of stainless steel construction mounted perpendicular to each other. Each chamber contains two gratings mounted at Littrow angle with the beam incident out-of-plane to enable input and output of the beam in the near-field. This configuration enables good access to the optics within the vessel for maintenance and alignment.

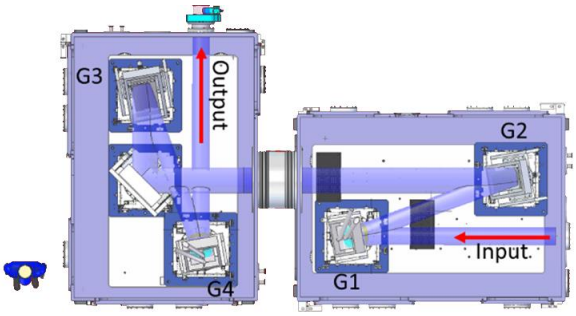

Figure 16: Overhead view of the two compressor vessels and the locations of the compressor gratings.

To optimally maintain the relative alignment between the surfaces of the gratings in the compressors, the grating mounts will stand on single piece breadboards that are then mounted onto the floor of the room through the compressor chamber. In this way they are isolated from any flexure of the compressor vessel as it is pumped down to vacuum. A common floorplate supports both the chambers and the breadboard support structure per sub-chamber, which to ensures even weight distribution onto the floor. Mechanical analysis has been performed during the design to ensure the chamber walls and flanges do not flex greater than a millimetre under vacuum load. Due to weight limitations of the reinforced second floor of the building, the design necessitates a structure that employs external strengthening ribs.

Diffraction Gratings

The technical challenges on grating technology are centred around achieving high diffractive efficiency across the broad 750-850 nm laser spectrum, high laser induced damage threshold (LIDT), and minimising the deformation of the grating surfaces from the high average power pulses. We have therefore decided to use gold coated diffraction gratings to achieve the LIDT and spectral coverage requirements. The fluence on the gratings has been designed to 80 mJ / cm^2, which is within a x2-3 safety factor to published LIDT on gold coated gratings and comparable to the laser fluence on the Gemini laser facility gratings [14],[16].

The grating dimensions are 300 x 300 mm for the first and last grating (G1, G4) and 300 x 760 mm for the intermediate gratings for the dispersed beam. The gratings will have a line density of 1480 l/mm and will be separated by 2 m in each sub-compressor. The G2, G3 grating size has been determined to capture the entire spectral content of the laser (Figure 17a) to minimise energy loss and spectral clipping effects that reduce pulse duration and degrade temporal contrast. The resultant spectrum from the combined amplification of the Front End and Ti:Sa amplifier is designed to produce a broad 65 nm FWHM pulse centred at 800 nm, with a Fourier-transform limited (FTL) duration of 21 fs FWHM.

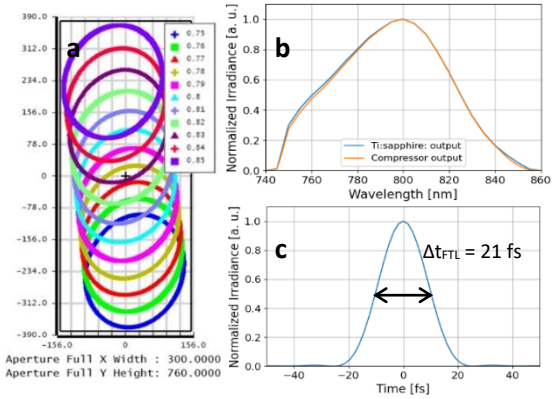

Figure 17: a) Spectral coverage on the large diffraction gratings (G2,G3). b) Modelled spectrum in and out of the EPAC compressor. c) Resultant Fourier-transform limited pulse duration of the compressor output bandwidth to be 21 fs.

At full spec, approximately 25 W of the 600 W average power of the laser will be absorbed by each grating substrate. When under vacuum, this slow heat absorption can eventually lead to grating surface deformations that would deleteriously degrade compressibility and focal spot quality onto experimental targets. The gratings substrates will therefore be a low coefficient of thermal expansion (CTE) glass-ceramic, such as Zerodur (Schott) or Clearceram-Z (Ohara), with up to twenty times lower CTE than fused silica. In this scheme, it will be possible to fire 1 Hz 1 PW pulses without detriment to compressibility and the possibility of a burst of 10 Hz laser shots, with the burst duration currently under analysis and determination likely decided during the commissioning of the system.

Input to Compressor

To maintain the laser fluence below the LIDT of the compressor gratings, an achromatic telescope, based on a Vulcan OPPEL design [13], will expand the 50 mm diameter output beam from the Ti:Sa amplifier to 220 mm. This achromatic telescope uses a positive and negative lens either side of a common focus of the to create an achromatic expanding beam. Finally, a parabolic mirror is placed for the large-aperture achromatic collimation with as little as ~λ/1000 achromatic error in wavefront collimation across the laser bandwidth.

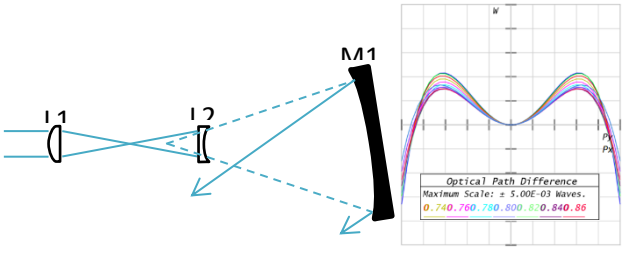

Figure 18: (Left) Schematic of the achromatic telescope for expansion to a 220mm beam to inject into the compressor, where $f_{L1} = -f_{L2}$. (Right) Optical path difference illustrating the wavefront aberrations, with chromatic aberrations reduced to the λ/1000 level.

The parabolic mirror will have a small, 2.5°, off-axis angle to expand the beam to 220 mm diameter that is sufficiently alignment insensitive for routine operations. Previous analysis has shown the collimation of the beam into the compressor must be precisely set to avoid ambiguities in spatial chirp and pulse length tuning [17]. The alignment of the parabola and expansion telescope will therefore be precisely set by turning the following mirror to a retro position and using diagnostics before the compressor.

Compressor Diagnostics

A further technical challenge surrounds the ability to characterise the compressed 30 J pulses without degrading the spatial and temporal characteristics of the pulse due to the B-integral. When firing shots at 10 Hz, on-shot continuous diagnostics will be critical to monitoring and compensation methods to counteract potential heating effects on the compressor optics and ensure long-term operational success at the highest repetition rate the facility can offer. A full aperture diagnostic beamline is therefore planned after the compressor.

The post-compressor diagnostics will use the leakage through a turning mirror. The beam will be magnified by two low-angle off-axis parabolas to 30 mm diameter under vacuum. Once the beam is collimated, it will be further attenuated using a series of glass blanks and a mirror, enabling a low energy low B-integral line and a high energy higher B-integral line. These beamlines will be extracted and imaged onto a diagnostics suite to characterise the compressed pulse. These include: near-field and dark-field monitoring of all gratings surfaces, far-field monitoring of the compressor output alignment, output wavefront, pulse front tilt, energy, spectrum, contrast and pulse duration and pulse dispersion diagnostics.

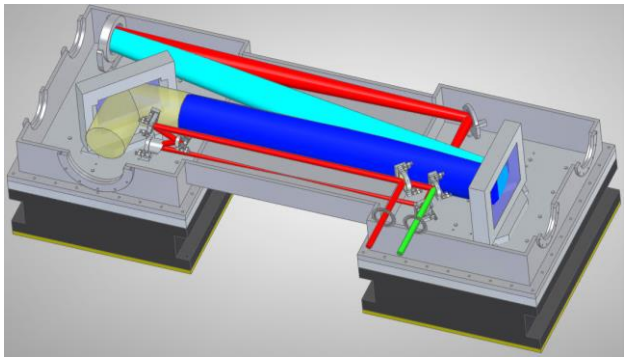

Figure 19. Schematic of the full beam diagnostics telescope to provide two channels of full aperture diagnostics.

Absolute calibration of the pulse duration measured in the full aperture diagnostics versus the main beamline will be achieved via a ~50 mm insertable pick-off of the central portion of the main beam that is only inserted for diagnostic setup.

Conclusions

The EPAC compressor geometry, optics and diagnostics aim to improve upon existing designs used in Astra Gemini and Vulcan. The high, 10Hz repetition rate of the facility poses unique optical and engineering challenges on the compressor stability and the need for reliable monitoring and control of laser pulses in real-time to ensure experiments that require multiple shots can be carried out. The installation of the chamber and optics is due to be complete in the middle of 2024.

References

[1] S. Banerjee, P. Mason, J. Phillips, et al. Pushing the boundaries of diode-pumped solid-state lasers for high-energy applications. High Power Laser Science and Engineering, 8 (2020) E20. https://doi.org/10.1017/hpl.2020.20

[2] I. Musgrave, W. Shaikh, M. Galimberti, A. Boyle, C. Hernandez-Gomez, K. Lancaster, R. Heathcote, Picosecond optical parametric chirped pulse amplifier as a preamplifier to generate high-energy seed pulses for contrast enhancement, Appl. Opt. 49 (2010) 6558–6562. https://doi.org/10.1364/AO.49.006558.

[3] D. Strickland, G. Mourou, Compression of Amplified Chirped Optical Pulses, Opt. Commun. 56 (1985) 219–221. https://doi.org/10.1016/0030-4018(85)90120-8.

[4] G. Archipovaite, M. Galletti, P. Oliveira, M. Galimberti, A. Frackiewicz, I. Musgrave, C. Hernandez-Gomez, 880 nm, 22 fs, 1 mJ pulses at 100 Hz as an OPCPA front end for Vulcan laser facility, Opt. Commun. 474 (2020) 126072. https://doi.org/10.1016/j.optcom.2020.126072.

[5] N.H. Stuart, D. Bigourd, R.W. Hill, T.S. Robinson, K. Mecseki, S. Patankar, G.H.C. New, R.A. Smith, Direct fluorescence characterisation of a picosecond seeded optical parametric amplifier, Opt. Commun. 336 (2015) 319–325. https://doi.org/10.1016/j.optcom.2014.09.032.

[6] N.V. Didenko, A.V. Konyashchenko, A.P. Lutsenko, S.Y. Tenyakov, Contrast degradation in a chirped-pulse amplifier due to generation of prepulses by postpulses, Opt. Express. 16 (2008) 3178. https://doi.org/10.1364/OE.16.003178.

[7] J. Zheng, H. Zacharias, Design considerations for a compact grism stretcher for non-collinear optical parametric chirped-pulse amplification, Appl. Phys. B. 96 (2009) 445–452. https://doi.org/10.1007/s00340-009-3410-6.

[8] Y. Tang, C. Hooker, O. Chekhlov, S. Hawkes, J. Collier, P.P. Rajeev, Transmission grating stretcher for contrast enhancement of high power lasers, Opt. Express. 22 (2014) 29363. https://doi.org/10.1364/OE.22.029363.

[9] S. Roeder, Y. Zobus, C. Brabetz, V. Bagnoud, How the laser beam size conditions the temporal contrast in pulse stretchers of chirped-pulse amplification lasers, High Power Laser Sci. Eng. 10 (2022) e34. https://doi.org/10.1017/hpl.2022.18.

[10] L. Ranc, C.L. Blanc, N. Lebas, L. Martin, J.-P. Zou, F. Mathieu, C. Radier, S. Ricaud, F. Druon, D. Papadopoulos, D. Papadopoulos, Improvement in the temporal contrast in the tens of ps range of the multi-PW Apollon laser front-end, Opt. Lett. 45 (2020) 4599–4602. https://doi.org/10.1364/OL.401272.

[11] C. J. Hooker et al, "The Astra Gemini Petawatt Ti:Sapphire Laser," The Review of Laser Engineering 37 (6), 443-448 (2009).

[12] M. Galimberti, I. Musgrave, A. Boyle, C. Hernandez-Gomez, T. Winstone, W. Shaikh, A. Wyatt, D. Pepler, I. Ross, A. Lyachev, J. Collier, Design Considerations for a High Energy Front-End for a High Power OPCPA Laser Facility, Rev. Laser Eng. 42 (2014) 137. https://doi.org/10.2184/lsj.42.2_137.

[13] M. Galletti, P. Oliveira, M. Galimberti, M. Ahmad, G. Archipovaite, N. Booth, E. Dilworth, A. Frackiewicz, T. Winstone, I. Musgrave, C. Hernandez-Gomez, Ultra-broadband all-OPCPA petawatt facility fully based on LBO, High Power Laser Sci. Eng. 8 (2020) e31. https://doi.org/10.1017/hpl.2020.31.

[14] C.J. Hooker, J.L. Collier, O. Chekhlov, R.J. Clarke, E.J. Divall, K. Ertel, P. Foster, S. Hancock, S.J. Hawkes, P. Holligan, A.J. Langley, W.J. Lester, D. Neely, B.T. Parry, B.E. Wyborn, The Astra Gemini Petawatt Ti:Sapphire Laser, 37 (2009) 443–448. https://doi.org/10.2184/lsj.37.443.

[15] D.A. Alessi, H.T. Nguyen, J.A. Britten, P.A. Rosso, C. Haefner, Low-dispersion low-loss dielectric gratings for efficient ultrafast laser pulse compression at high average powers, Opt. Laser Technol. 117 (2019) 239–243. https://doi.org/10.1016/j.optlastec.2019.04.005

[16] P. Poole, S. Trendafilov, G. Shvets, D. Smith, E. Chowdhury, Femtosecond laser damage threshold of pulse compression gratings for petawatt scale laser systems, Opt. Express. 21 (2013) 26341–26351. https://doi.org/10.1364/OE.21.026341.

[17] R. Heathcote, M. Galimberti, R.J. Clarke, T.B. Winstone, I.O. Musgrave, C. Hernandez-Gomez, Collimation effects on large CPA compressors, Appl. Phys. B. 116 (2014) 805–809. https://doi.org/10.1007/s00340-014-5765-6.